



HAL
open science

Unsteady flow of a fourth grade fluid due to an oscillating plate

Yongqi Wang, Wei Wu

► **To cite this version:**

Yongqi Wang, Wei Wu. Unsteady flow of a fourth grade fluid due to an oscillating plate. *International Journal of Non-Linear Mechanics*, 2007, 42 (3), pp.432. 10.1016/j.ijnonlinmec.2007.01.003 . hal-00501741

HAL Id: hal-00501741

<https://hal.science/hal-00501741>

Submitted on 12 Jul 2010

HAL is a multi-disciplinary open access archive for the deposit and dissemination of scientific research documents, whether they are published or not. The documents may come from teaching and research institutions in France or abroad, or from public or private research centers.

L'archive ouverte pluridisciplinaire **HAL**, est destinée au dépôt et à la diffusion de documents scientifiques de niveau recherche, publiés ou non, émanant des établissements d'enseignement et de recherche français ou étrangers, des laboratoires publics ou privés.

Author's Accepted Manuscript

Unsteady flow of a fourth grade fluid due to an oscillating plate

Yongqi Wang, Wei Wu

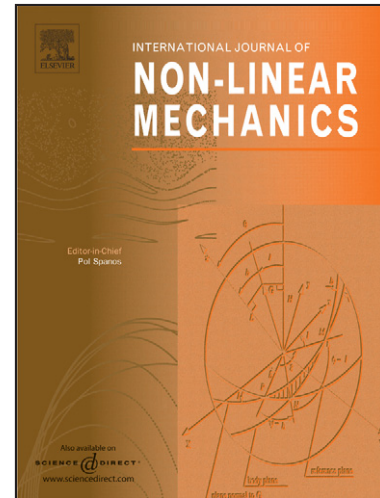
PII: S0020-7462(07)00036-4
DOI: doi:10.1016/j.ijnonlinmec.2007.01.003
Reference: NLM 1321

To appear in: *International Journal of Non-Linear Mechanics*

Received date: 19 May 2006
Revised date: 17 August 2006
Accepted date: 6 January 2007

Cite this article as: Yongqi Wang and Wei Wu, Unsteady flow of a fourth grade fluid due to an oscillating plate, *International Journal of Non-Linear Mechanics* (2007), doi:10.1016/j.ijnonlinmec.2007.01.003

This is a PDF file of an unedited manuscript that has been accepted for publication. As a service to our customers we are providing this early version of the manuscript. The manuscript will undergo copyediting, typesetting, and review of the resulting galley proof before it is published in its final citable form. Please note that during the production process errors may be discovered which could affect the content, and all legal disclaimers that apply to the journal pertain.



www.elsevier.com/locate/nlm

Unsteady Flow of a Fourth Grade Fluid Due to an Oscillating Plate

Yongqi Wang^{1,2} and Wei Wu¹

*1. Institute of Geotechnical Engineering
University of Natural Resources & Applied Life Sciences
Feistmantelstr. 4, 1180 Vienna, Austria*

*2. Chair of Fluid Dynamics, Department of Mechanical Engineering
Darmstadt University of Technology, Hochschulstrasse 1, 64289 Darmstadt, Germany
wang@fdy.tu-darmstadt.de*

Abstract

The governing non-linear high-order, sixth-order in space and third-order in time, differential equation is constructed for the unsteady flow of an incompressible conducting fourth-grade fluid in a semi-infinite domain. The unsteady flow is induced by a periodically oscillating two-dimensional infinite porous plate with suction/blowing, located in a uniform magnetic field. It is shown that by augmenting additional boundary conditions at infinity based on asymptotic structures and transforming the semi-infinite physical space to a bounded computational domain by means of a coordinate transformation, it is possible to obtain numerical solutions of the nonlinear magnetohydrodynamic equation. In particular, due to the unsymmetry of the boundary conditions, in numerical simulations non-central difference schemes are constructed and employed to approximate the emerging higher-order spatial derivatives. Effects of material parameters, uniform suction or blowing past the porous plate, exerted magnetic field and oscillation frequency of the plate on the time-dependent flow, especially on the boundary layer structure near the plate, are numerically analysed and discussed. The flow behaviour of the fourth-grade non-Newtonian fluid is also compared with those of the Newtonian fluid.

Key words: Fourth-grade fluid; non-Newtonian fluid; magnetohydrodynamic fluid; time-dependent flow.

1 Introduction

The inadequacy of the classical Navier-Stokes theory to describe rheologically complex fluids such as polymer solutions, blood, paints, certain oils and greases, has led to the

development of several theories of non-Newtonian fluids. In recent years, amongst the many models which have been used to describe the non-Newtonian behaviours exhibited by certain fluids, the fluids of differential type [16] have received special attention, as well as much controversy, see e.g. [5] for a complete discussion of the relevant issues. The fluids of second and third grade, which form a subclass of the fluids of the differential type, have been studied successfully in various types of flow situations. We mention here some of the studies such as Akyildiz [1], Benharbit and Siddiqui [3], Erdogan [6], Gupta and Massoudi [7], Hayat et. al. [8, 9] and Rajagopal [14].

Although the second-grade model is found to predict the normal stress differences, it does not properly respond to shear thinning or thickening due to its constant apparent shear viscosity. For this reason, some experiments may be well described by the fluids of grade three or four [2, 4, 11]. Keeping this fact in view, the aim of the present analysis is to venture further into the regime of fourth-grade fluids. Only fairly scarce literatures are available [10, 12, 17]. No attempt has been made to model unsteady flows of fourth-grade fluids in the context of magnetohydrodynamics. In the present analysis, such an attempt is made. Literature survey reveals no previous attempts at studying such a high-order nonlinear partial differential equation even in the absence of plate porosity and magnetic field. The modelled partial differential equation is in a generalized form and is a significant contribution to understand the behaviour of fourth-grade fluids both from physical and mathematical standpoints. We examine numerically the unsteady flow in a semi-infinite space caused by the periodic motion of an infinite plate. In solving this problem the additional boundary conditions that are imposed at infinity are of particular interest. Furthermore, by a coordinate transformation, the flow problem needs to be solved only in a bounded computational domain instead of the investigated semi-infinite physical space. Due to the inequality of the numbers of the boundary conditions at both boundaries, i.e., much more boundary conditions at infinity than at the plate, in numerical simulations non-central difference schemes are constructed and employed to approximate the emerging higher-order spatial derivatives. These difference schemes are inclined toward the boundary at infinity and but still of second-order accuracy. The effects of the material parameters of the fourth-grade fluid, magnetic field and suction through the plate on the velocity spatial distribution and its time series are investigated and compared with the Newtonian fluid.

2 Equation of Motion

The basic field equations governing the flow of an incompressible conducting fluid are

$$\operatorname{div} \mathbf{v} = 0, \quad (1)$$

$$\rho \frac{d\mathbf{v}}{dt} = \operatorname{div} \mathbf{T} + \mathbf{J} \times \mathbf{B}, \quad (2)$$

where ρ is the density, \mathbf{v} the velocity, \mathbf{T} the Cauchy stress tensor, \mathbf{J} the current density and \mathbf{B} the total magnetic field so that $\mathbf{B} = \mathbf{B}_0 + \mathbf{b}$, \mathbf{b} is the induced magnetic field. d/dt denotes the material time derivative.

The above system of equations will be closed by a constitutive equation for the stress tensor \mathbf{T} . We examine the flow of an incompressible fourth-grade fluid described by the

constitutive equation

$$\mathbf{T} = -p\mathbf{I} + \sum_{j=1}^n \mathbf{S}_j \quad (3)$$

with $n = 4$, in which

$$\mathbf{S}_1 = \mu \mathbf{A}_1, \quad (4)$$

$$\mathbf{S}_2 = \alpha_1 \mathbf{A}_2 + \alpha_2 \mathbf{A}_1^2, \quad (5)$$

$$\mathbf{S}_3 = \beta_1 \mathbf{A}_3 + \beta_2 (\mathbf{A}_1 \mathbf{A}_2 + \mathbf{A}_2 \mathbf{A}_1) + \beta_3 (\text{tr } \mathbf{A}_1^2) \mathbf{A}_1, \quad (6)$$

$$\begin{aligned} \mathbf{S}_4 = & \gamma_1 \mathbf{A}_4 + \gamma_2 (\mathbf{A}_3 \mathbf{A}_1 + \mathbf{A}_1 \mathbf{A}_3) + \gamma_3 \mathbf{A}_2^2 + \gamma_4 (\mathbf{A}_2 \mathbf{A}_1^2 + \mathbf{A}_1^2 \mathbf{A}_2) \\ & + \gamma_5 (\text{tr } \mathbf{A}_2) \mathbf{A}_2 + \gamma_6 (\text{tr } \mathbf{A}_2) \mathbf{A}_1^2 + [\gamma_7 \text{tr } \mathbf{A}_3 + \gamma_8 \text{tr } (\mathbf{A}_2 \mathbf{A}_1)] \mathbf{A}_1, \end{aligned} \quad (7)$$

where μ is the coefficient of shear viscosity, and α_i ($i = 1, 2$), β_i ($i = 1, 2, 3$), γ_i ($i = 1, 2, \dots, 8$) are material parameters. The Rivlin-Ericksen tensors \mathbf{A}_n are defined by the recursion relation:

$$\begin{aligned} \mathbf{A}_n &= \frac{d\mathbf{A}_{n-1}}{dt} + \mathbf{A}_{n-1}(\text{grad } \mathbf{v}) + (\text{grad } \mathbf{v})^T \mathbf{A}_{n-1}, \quad n > 1, \\ \mathbf{A}_1 &= (\text{grad } \mathbf{v}) + (\text{grad } \mathbf{v})^T. \end{aligned} \quad (8)$$

We note that when $\gamma_i = 0$ ($i = 1, 2, \dots, 8$) the fourth-grade model reduces to the third-grade model, i.e., $n = 3$ in (3), while when $\beta_i = 0$ ($i = 1, 2, 3$) and $\gamma_i = 0$ ($i = 1, 2, \dots, 8$) the model reduces to a second-grade fluid, corresponding to the case of $n = 2$ in (3). If all of the high-order material parameters vanish, i.e., $\alpha_i = 0$ ($i = 1, 2$), $\beta_i = 0$ ($i = 1, 2, 3$) and $\gamma_i = 0$ ($i = 1, 2, \dots, 8$), the model reduces to the classical Navier-Stokes fluid.

We consider the unsteady flow of the incompressible, conducting fourth-grade fluid, excited by the longitudinal oscillation of an infinite porous plate with suction/blowing. We employ a spatial coordinate system with the origin on the plate, x -axis along the plate in the direction of the plate movement, and y -axis perpendicular to the plate directed toward the fluid, which is in contact with the plate and occupies the whole semi-infinite region $y \geq 0$. A uniform magnetic field $\mathbf{B}_0 = B_0 \mathbf{k}$ (\mathbf{k} is a unit vector normal to the plate in the y -direction) is applied to the fluid system. In the low-magnetic-Reynolds-number approximation, in which the induced magnetic field \mathbf{b} can be ignored, the magnetic body force becomes (see e.g. [18])

$$\mathbf{J} \times \mathbf{B} = -\sigma B_0^2 \mathbf{v}, \quad (9)$$

in which σ is the electrical conductivity of the fluid.

Under these conditions, the flow is independent of x . Thus, it follows from the equation of continuity (1) that

$$\frac{\partial v}{\partial y} = 0, \quad (10)$$

hence the velocity component in y -direction, v , is a function of time only. We take

$$v = \text{const} = -v_0, \quad (11)$$

where v_0 is the suction ($v_0 > 0$) and blowing ($v_0 < 0$) velocity normal to the plate.

We shall seek a velocity field of the form

$$\mathbf{v} = (u, v, w) = (u(y, t), -v_0, 0), \quad (12)$$

where u , v and w are the x , y and z components of the velocity field.

Substituting (4)–(8), (11) and (12) into (3), then the resulting constitutive relations together with (9) again into the momentum equation (2), and subsequently eliminating the emerging pressure gradients $\partial p/\partial x$ and $\partial p/\partial y$ by cross differentiation, after some intricate computations, we can obtain a differential equation

$$\begin{aligned} & \rho \left[\frac{\partial^2 u}{\partial y \partial t} - v_0 \frac{\partial^2 u}{\partial y^2} \right] \\ = & \mu \frac{\partial^3 u}{\partial y^3} - \sigma B_0^2 \frac{\partial u}{\partial y} + \alpha_1 \left(\frac{\partial^4 u}{\partial y^3 \partial t} - v_0 \frac{\partial^4 u}{\partial y^4} \right) + \beta_1 \left(\frac{\partial^5 u}{\partial y^3 \partial t^2} - 2v_0 \frac{\partial^5 u}{\partial y^4 \partial t} + v_0^2 \frac{\partial^5 u}{\partial y^5} \right) \\ & + 6(\beta_2 + \beta_3) \frac{\partial}{\partial y} \left\{ \left(\frac{\partial u}{\partial y} \right)^2 \frac{\partial^2 u}{\partial y^2} \right\} + \gamma_1 \left(\frac{\partial^6 u}{\partial y^3 \partial t^3} - 3v_0 \frac{\partial^6 u}{\partial y^4 \partial t^2} + 3v_0^2 \frac{\partial^6 u}{\partial t \partial y^5} - v_0^3 \frac{\partial^6 u}{\partial y^6} \right) \\ & + (6\gamma_2 + 2\gamma_3 + 2\gamma_4 + 2\gamma_5 + 6\gamma_7 + 2\gamma_8) \frac{\partial^2}{\partial y^2} \left(\left(\frac{\partial u}{\partial y} \right)^2 \left(\frac{\partial^2 u}{\partial y \partial t} - v_0 \frac{\partial^2 u}{\partial y^2} \right) \right). \quad (13) \end{aligned}$$

Its dimensionless form can be written as

$$\begin{aligned} & \frac{\partial}{\partial \bar{t}} \left\{ \frac{\partial \bar{u}}{\partial \bar{y}} - \bar{\alpha}_1 \frac{\partial^3 \bar{u}}{\partial \bar{y}^3} + 2\bar{\beta}_1 \bar{v}_0 \frac{\partial^4 \bar{u}}{\partial \bar{y}^4} - 3\bar{\gamma}_1 \bar{v}_0^2 \frac{\partial^5 \bar{u}}{\partial \bar{y}^5} \right\} - 2\bar{\gamma} \left[\left(\frac{\partial^2 \bar{u}}{\partial \bar{y}^2} \right)^2 + \frac{\partial \bar{u}}{\partial \bar{y}} \frac{\partial^3 \bar{u}}{\partial \bar{y}^3} \right] \frac{\partial}{\partial \bar{t}} \left\{ \frac{\partial \bar{u}}{\partial \bar{y}} \right\} \\ & - 4\bar{\gamma} \frac{\partial \bar{u}}{\partial \bar{y}} \frac{\partial^2 \bar{u}}{\partial \bar{y}^2} \frac{\partial}{\partial \bar{t}} \left\{ \frac{\partial^2 \bar{u}}{\partial \bar{y}^2} \right\} - \bar{\gamma} \left(\frac{\partial \bar{u}}{\partial \bar{y}} \right)^2 \frac{\partial}{\partial \bar{t}} \left\{ \frac{\partial^3 \bar{u}}{\partial \bar{y}^3} \right\} \\ & + \frac{\partial^2}{\partial \bar{t}^2} \left\{ 3\bar{\gamma}_1 \bar{v}_0 \frac{\partial^4 \bar{u}}{\partial \bar{y}^4} - \bar{\beta}_1 \frac{\partial^3 \bar{u}}{\partial \bar{y}^3} \right\} - \bar{\gamma}_1 \frac{\partial^3}{\partial \bar{t}^3} \left\{ \frac{\partial^3 \bar{u}}{\partial \bar{y}^3} \right\} \\ = & -\bar{B} \frac{\partial \bar{u}}{\partial \bar{y}} + \bar{v}_0 \frac{\partial^2 \bar{u}}{\partial \bar{y}^2} + \frac{\partial^3 \bar{u}}{\partial \bar{y}^3} - \bar{\alpha}_1 \bar{v}_0 \frac{\partial^4 \bar{u}}{\partial \bar{y}^4} + \bar{\beta}_1 \bar{v}_0^2 \frac{\partial^5 \bar{u}}{\partial \bar{y}^5} + \bar{\beta} \left(2 \frac{\partial \bar{u}}{\partial \bar{y}} \left(\frac{\partial^2 \bar{u}}{\partial \bar{y}^2} \right)^2 + \left(\frac{\partial \bar{u}}{\partial \bar{y}} \right)^2 \frac{\partial^3 \bar{u}}{\partial \bar{y}^3} \right) \\ & - \bar{\gamma}_1 \bar{v}_0^3 \frac{\partial^6 \bar{u}}{\partial \bar{y}^6} - \bar{\gamma} \bar{v}_0 \left(2 \left(\frac{\partial^2 \bar{u}}{\partial \bar{y}^2} \right)^3 + 6 \frac{\partial \bar{u}}{\partial \bar{y}} \frac{\partial^2 \bar{u}}{\partial \bar{y}^2} \frac{\partial^3 \bar{u}}{\partial \bar{y}^3} + \left(\frac{\partial \bar{u}}{\partial \bar{y}} \right)^2 \frac{\partial^4 \bar{u}}{\partial \bar{y}^4} \right), \quad (14) \end{aligned}$$

where the emerging dimensionless variables and parameters are defined by

$$\begin{aligned} \bar{u} &= \frac{u}{U}, \quad \bar{y} = \frac{Uy}{\nu}, \quad \bar{v}_0 = \frac{v_0}{U}, \quad \bar{t} = \frac{\rho U^2}{\mu} t, \\ \bar{B} &= \frac{\nu \sigma B_0^2}{\rho U^2}, \quad \bar{\alpha}_1 = \frac{\alpha_1 U^2}{\rho \nu^2}, \quad \bar{\beta}_1 = \frac{\beta_1 U^4}{\rho \nu^3}, \quad \bar{\gamma}_1 = \frac{\gamma_1 U^6}{\rho \nu^4}, \\ \bar{\beta} &= \frac{6(\beta_2 + \beta_3) U^4}{\rho \nu^3}, \quad \bar{\gamma} = 2(3\gamma_2 + \gamma_3 + \gamma_4 + \gamma_5 + 3\gamma_7 + \gamma_8) \frac{U^6}{\rho \nu^4}, \end{aligned} \quad (15)$$

in which U is a reference velocity and $\nu = \mu/\rho$ is the fluid kinematic viscosity.

We note that (14) is a high-order partial differential equation (sixth-order in space and third-order in time) and thus requires additional boundary conditions except for the usual boundary conditions for a Newtonian fluid [15]. As we are solving the problem in an unbounded domain, it is possible to augment the boundary conditions by enforcing additional asymptotic structures at infinity. Here, we augment the additional boundary conditions by requiring that the several high-order derivatives in space vanish at infinity. Similar additional initial conditions are also postulated. Their different choices may have influence only on the numerical results for the initial time steps. We will solve (14) in the domain $\bar{y} \in [0, \infty)$ with the following boundary conditions

$$\begin{aligned} \bar{u} &= \sin(\bar{\omega}\bar{t}) && \text{at } \bar{y} = 0, \\ \bar{u} &= 0, \quad \frac{\partial^n \bar{u}}{\partial \bar{y}^n} = 0 \quad (n = 2, 3, 4, 5) && \text{at } \bar{y} \rightarrow \infty, \end{aligned} \quad (16)$$

and the initial conditions

$$\bar{u} = 0, \quad \frac{\partial^n \bar{u}}{\partial \bar{t}^n} = 0, \quad (n = 2, 3) \quad \text{at } \bar{t} = 0. \quad (17)$$

For the boundary condition at the plate, (16)₁, we assume a non-slip condition and the plate oscillates in a sinusoidal form, in which $\bar{\omega}$ is the corresponding dimensionless frequency. It should be pointed out that the additional boundary conditions at $\bar{y} \rightarrow \infty$ in (16)₂ are specified for $n = 2, 3, 4, 5$ instead of those for $n = 1, 2, 3, 4$. This choice is for no other reason than the consideration of numerical simulations, because the physical value at the first interior grid point near the boundary $\bar{y} \rightarrow \infty$ would be determined directly by the boundary conditions instead of the governing differential equation, if the other choice with $n = 1, 2, 3, 4$ would be employed. It is also the similar case for the additional initial conditions (17)₂.

For simplicity, in the following we will drop the bars of the dimensionless variables.

3 Numerical Method

Approximate solutions can be obtained by truncating the semi-infinite domain. In this approximation, the semi-infinite domain $y \in [0, \infty)$ is replaced by a finite domain $y \in [0, H]$ and the boundary conditions at infinity $y \rightarrow \infty$ are enforced at $y = H$. The length H is chosen in such a manner that any further increase in its value does not significantly alter the solution. It should be emphasized here that proper care should be exercised in the determination of the solution because it is well known that even in the case of a Navier-Stokes fluid spurious solutions are possible due to the truncation of an infinite domain to a bounded one [13].

In order to avoid such possible spurious solutions, in this paper the coordinate transformation $\eta = 1/(y + 1)$ is applied to transform the semi-infinite physical domain $y \in [0, \infty)$ to a finite calculation domain $\eta \in [0, 1]$, by the following transformation relations

$$y = \frac{1}{\eta} - 1, \quad \frac{\partial}{\partial y} = -\eta^2 \frac{\partial}{\partial \eta}, \quad \frac{\partial^2}{\partial y^2} = \eta^4 \frac{\partial^2}{\partial \eta^2} + 2\eta^3 \frac{\partial}{\partial \eta},$$

$$\begin{aligned}
\frac{\partial^3}{\partial y^3} &= -\eta^6 \frac{\partial^3}{\partial \eta^3} - 6\eta^5 \frac{\partial^2}{\partial \eta^2} - 6\eta^4 \frac{\partial}{\partial \eta}, \\
\frac{\partial^4}{\partial y^4} &= \eta^8 \frac{\partial^4}{\partial \eta^4} + 12\eta^7 \frac{\partial^3}{\partial \eta^3} + 36\eta^6 \frac{\partial^2}{\partial \eta^2} + 24\eta^5 \frac{\partial}{\partial \eta}, \\
\frac{\partial^5}{\partial y^5} &= -\eta^{10} \frac{\partial^5}{\partial \eta^5} - 20\eta^9 \frac{\partial^4}{\partial \eta^4} - 120\eta^8 \frac{\partial^3}{\partial \eta^3} - 240\eta^7 \frac{\partial^2}{\partial \eta^2} - 120\eta^6 \frac{\partial}{\partial \eta}, \\
\frac{\partial^6}{\partial y^6} &= \eta^{12} \frac{\partial^6}{\partial \eta^6} + 30\eta^{11} \frac{\partial^5}{\partial \eta^5} + 300\eta^{10} \frac{\partial^4}{\partial \eta^4} + 1200\eta^9 \frac{\partial^3}{\partial \eta^3} + 1800\eta^8 \frac{\partial^2}{\partial \eta^2} + 720\eta^7 \frac{\partial}{\partial \eta}.
\end{aligned} \tag{18}$$

With these transformations, the governing differential equation (14) can be rewritten in the η coordinate. Here, we avoid writing its explicit form because of its complexity. The boundary conditions (16) in terms of η can be rewritten as

$$\begin{aligned}
u &= \sin(\omega t), & \text{at } \eta &= 1, \\
u &= 0, \quad \frac{\partial^n u}{\partial \eta^n} = 0 \quad (n = 2, 3, 4, 5), & \text{at } \eta &= 0.
\end{aligned} \tag{19}$$

In the subsequent simulations for most cases the dimensionless oscillation frequency of the plate, ω , is simply taken as $\omega = 1$, but we will also discuss the effect of various values of ω on the time series of velocity and the structure of the boundary layer near plate.

The differential equation (14) is a nonlinear high-order differential equation. We can solve this initial-boundary value problem (14), (17) and (19) by finite difference method. We can discretize (14) (in fact its form in terms of η) for M uniformly distributed discrete points $\eta = (\eta_1, \eta_2, \dots, \eta_M) \in (0, 1)$ with a space grid size of $\Delta\eta = 1/(M + 1)$ and time steps $t = (t^{(1)}, t^{(2)}, \dots, t^{(n)}, \dots) = (\Delta t, 2\Delta t, \dots, n\Delta t, \dots)$, where Δt is the time step size. Due to the inequality of the numbers of the boundary conditions at both boundaries, i.e., five conditions at $\eta = 0$, but only one at $\eta = 1$, we cannot use central differences to approximate the high-order derivatives emerging in (14) and (19) (if the order > 2). The following finite difference schemes are constructed and employed for different order derivatives. Except for the first and second derivatives they are not central differences, but inclined towards the boundary $\eta = 0$, where more boundary conditions are specified; however they are still of second-order accuracy. Here, we omit the laborious derivation and only list the formulas for the derivatives at point $\eta = \eta_j$:

$$\begin{aligned}
\frac{\partial u}{\partial \eta} \Big|_{\eta=\eta_j} &= \frac{u_{j+1} - u_{j-1}}{2(\Delta\eta)} + o(\Delta\eta^2), \\
\frac{\partial^2 u}{\partial \eta^2} \Big|_{\eta=\eta_j} &= \frac{u_{j+1} - 2u_j + u_{j-1}}{(\Delta\eta)^2} + o(\Delta\eta^2), \\
\frac{\partial^3 u}{\partial \eta^3} \Big|_{\eta=\eta_j} &= \frac{3u_{j+1} - 10u_j + 12u_{j-1} - 6u_{j-2} + u_{j-3}}{2(\Delta\eta)^3} + o(\Delta\eta^2), \\
\frac{\partial^4 u}{\partial \eta^4} \Big|_{\eta=\eta_j} &= \frac{2u_{j+1} - 9u_j + 16u_{j-1} - 14u_{j-2} + 6u_{j-3} - u_{j-4}}{(\Delta\eta)^4} + o(\Delta\eta^2),
\end{aligned} \tag{20}$$

$$\begin{aligned}\frac{\partial^5 u}{\partial \eta^5} \Big|_{\eta=\eta_j} &= \frac{5u_{j+1} - 28u_j + 65u_{j-1} - 80u_{j-2} + 55u_{j-3} - 20u_{j-4} + 3u_{j-5}}{2(\Delta\eta)^5} + o(\Delta\eta^2), \\ \frac{\partial^6 u}{\partial \eta^6} \Big|_{\eta=\eta_j} &= \frac{3u_{j+1} - 20u_j + 57u_{j-1} - 90u_{j-2} + 85u_{j-3} - 48u_{j-4} + 15u_{j-5} - 2u_{j-6}}{(\Delta\eta)^6} \\ &\quad + o(\Delta\eta^2),\end{aligned}$$

in which $o(\Delta\eta^2)$ denotes quantities which are higher order small than $\Delta\eta^2$.

For the fifth-order derivative emerging in the boundary condition at infinity $\eta = 0$ ($j = 0$) and the sixth-order derivative emerging in the differential equation (14) for the first interior grid point near the boundary of infinity $\eta = 0$ ($j = 1$) only difference approximations with first-order accuracy are used to avoid additional unknown imaginary boundary values, i.e.,

$$\begin{aligned}\frac{\partial^5 u}{\partial \eta^5} \Big|_{\eta=\eta_j} &= \frac{u_{j+1} - 5u_j + 10u_{j-1} - 10u_{j-2} + 5u_{j-3} - u_{j-4}}{(\Delta\eta)^5} + o(\Delta\eta), \quad (j = 0) \\ \frac{\partial^6 u}{\partial \eta^6} \Big|_{\eta=\eta_j} &= \frac{u_{j+1} - 6u_j + 15u_{j-1} - 20u_{j-2} + 15u_{j-3} - 6u_{j-4} + u_{j-5}}{(\Delta\eta)^6} \\ &\quad + o(\Delta\eta) \quad (j = 1).\end{aligned}\tag{21}$$

Similarly, a temporally afterwards form for the third-order time derivative is used

$$\frac{\partial^3 u}{\partial t^3} \Big|_{t=t^{(n)}} = \frac{3u^{(n+1)} - 10u^{(n)} + 12u^{(n-1)} - 6u^{(n-2)} + u^{(n-3)}}{2(\Delta t)^3} + o(\Delta t^2),\tag{22}$$

whilst for the first- and second-order time derivative still traditional central difference schemes are employed.

In so doing, for each time step a linear algebraic equation system emerges. Its coefficient matrix has a bandwidth of eight elements. This equation system can be solved e.g. by Gaussian elimination. The values of the velocity field u at the boundary points $\eta_0 = 0$ ($j = 0$), $\eta_{M+1} = 1$ ($j = M + 1$) and the imaginary points outside the domain ($j = -1, -2, -3, -4$) can be obtained by using the boundary conditions (19).

4 Numerical Results and Discussions

We compare the velocity profiles for two kinds of fluids: the Newtonian fluid, for which $\alpha_1 = 0$, $\beta = \beta_1 = 0$ and $\gamma = \gamma_1 = 0$, and the full fourth-grade non-Newtonian fluid, in which for most cases we choose $\alpha_1 = \beta_1 = \beta = \gamma_1 = \gamma = 1$ without physical reasons. In addition the influences of other different values of the material parameters are also investigated. In order to clearly observe the structure of the boundary layer near the plate, all numerical results are depicted in the y -coordinate only for a truncated physical domain $y \in [0, 9]$ (corresponding to $\eta \in [0.1, 1]$) near the plate, after finishing the simulations in the whole computational domain $\eta \in [0, 1]$, corresponding to the physical domain $z \in [0, \infty)$.

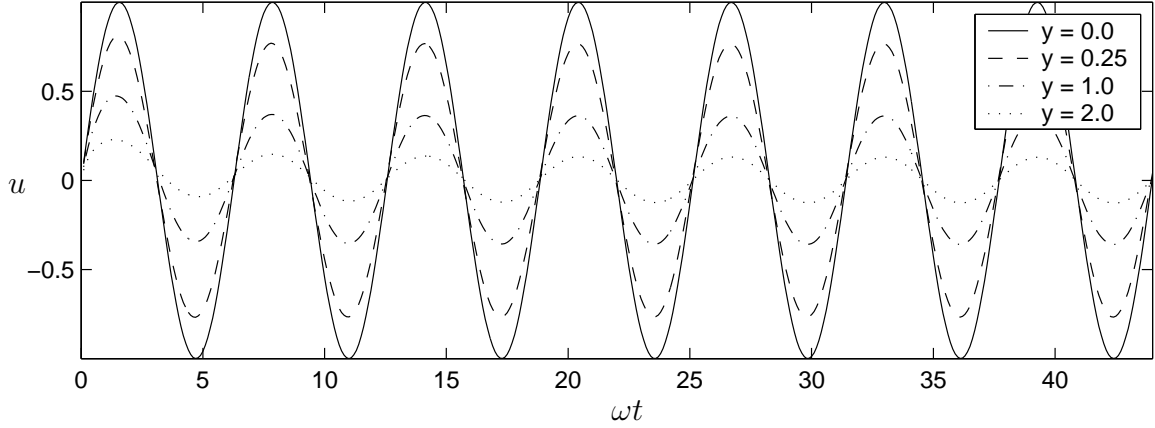


Figure 1: Time series of the flow velocity at several different distances from the plate $y = 0, 0.25, 1.0, 2.0$ within the first seven periods $\omega t \in [0, 14\pi]$ for the fourth-grade non-Newtonian fluid with the chosen material parameters $\alpha_1 = \beta = \beta_1 = \gamma = \gamma_1 = 1$. The other parameters are chosen as $B = 0, v_0 = 0$ and $\omega = 1$.

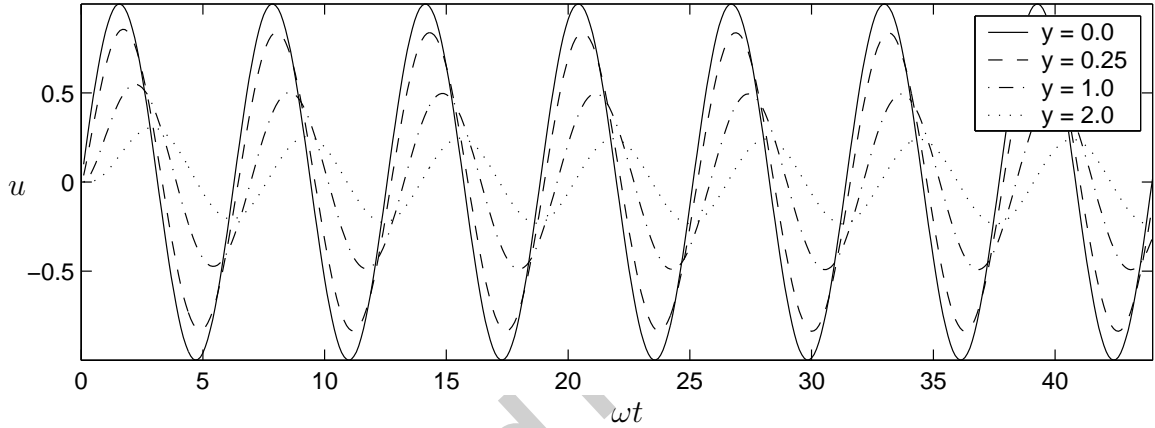


Figure 2: Time series of the flow velocity at several different distances from the plate $y = 0, 0.25, 1.0, 2.0$ within the first seven periods $\omega t \in [0, 14\pi]$ for the Newtonian fluid, for which $\alpha_1 = \beta = \beta_1 = \gamma = \gamma_1 = 0$. The other parameters are chosen as $B = 0, v_0 = 0$ and $\omega = 1$.

The time series of the flow velocity in several different positions (different distances from the plate) for the first seven periods $\omega t \in [0, 14\pi]$ are displayed in Fig. 1 for the fourth-grade non-Newtonian fluid and in Fig. 2 for the Newtonian fluid, respectively. Obviously, periodic flows can be reached almost immediately after the set-up of the flow conditions, at most after two periods. Due to the no-slip boundary condition at the solid boundary the fluid near the plate oscillates together with the plate in the same phase and the amplitude. The velocity amplitude decays rapidly with the increase of the distance from the plate. Whilst the flow of the fourth-grade non-Newtonian fluid in the whole flow domain oscillates approximately in phase with the driving plate movement (Fig. 1), a phase lag behind the excitation occurs for the Newtonian fluid which increases with the increase of the distance away from the plate (Fig. 2). Actually, these phase difference

depends on the ratio of viscous to inertial forces for the investigated fluids. If the apparent viscosity of the fluid is sufficiently large, i.e., the viscous forces dominate, the flow can simultaneously adapt to the current driving force and oscillates approximately with the same phase in the whole flow domain. This is the case for the fourth-order non-Newtonian fluid. For the Newtonian fluid displayed in Fig. 2 the inertial forces dominate and the flow slowly reacts to the changes of the plate movement, hence in the flow velocity a phase lag behind the excitation occurs. This time delay increases with the increase of the distance from the plate.

From Figs. 3 and 4 it can be clearly seen that the investigated fourth-grade non-Newtonian fluid shows a larger apparent viscosity than the corresponding Newtonian fluid. In both figures the velocity profiles at two different phases $\omega t = (2n + 1/2)\pi$ (wave peak) and $\omega t = (2n + 3/2)\pi$ (wave trough) within a period $\omega t \in [2n\pi, 2(n + 1)\pi]$ with a sufficiently large value of n , for which the periodic flow has been reached (e.g. after several periods), are represented for various values of the second-order (α_1) in Fig. 3 and third-order material parameters (β, β_1) in Fig. 4 of the non-Newtonian fluid, respectively. For comparison, the corresponding velocity profiles of the Newtonian fluid are also displayed (solid lines in the figures). In general, the non-Newtonian fluid exhibits a much thicker boundary layer, indicating a larger apparent viscosity than that of the Newtonian fluid. Increasing these second- and third-order material parameters (α_1 in Fig. 3 and β, β_1 in Fig. 4) causes further thickening of the boundary layer. Furthermore, increasing the fourth-order material parameters, γ and γ_1 , indicates a similar tendency, that is for brevity not shown here.

The numerical results obtained by using various suction velocities v_0 through the plate are illustrated in Fig. 5. The alteration tendencies of the velocity distributions by varying v_0 are practically converse for the Newtonian fluid and the fourth-grade fluid. For the Newtonian fluid (Fig. 5a), when the suction velocity v_0 increases, as one may expect, the boundary layer near the plate ($y = 0$) tends to become thinner. On the contrary, for the fourth-order fluid (Fig. 5b) the effect of increase in the suction velocity increases the boundary layer thickness. Test computations with other different high-order material parameters show similar tendency, except when all high-order material parameters are chosen to be very small, for which the fourth-grade fluid behaves like a Newtonian fluid. In general, the boundary layer for the Newtonian fluid is much thinner than that for the fourth-order fluid, especially for the case with a suction through the porous plate. For a blowing through the plate, the fluids behave qualitatively opposite to a suction velocity. In this case, with the increase of the blowing velocity, for the Newtonian fluid the shear boundary layer becomes thicker rapidly, whilst for the fourth-grade fluids the thickness of boundary layers is not so sensitive to variations in the blowing, and only slight thinning of the boundary layer occurs. To save space, the corresponding results with a blowing are not graphically displayed.

The dependence of the distributions of the flow velocity on the magnetic field is shown in Fig. 6. An applied magnetic field tends to restrict the shearing to a thinner boundary layer near the plate not only for the investigated fourth-order non-Newtonian fluid but also for the Newtonian fluid, although this thinning seems to be more obvious for the fourth-order fluid than that of the Newtonian fluid. The reason for this thinning is that the magnetic field provides a resistance to the flow and hence decrease the flow

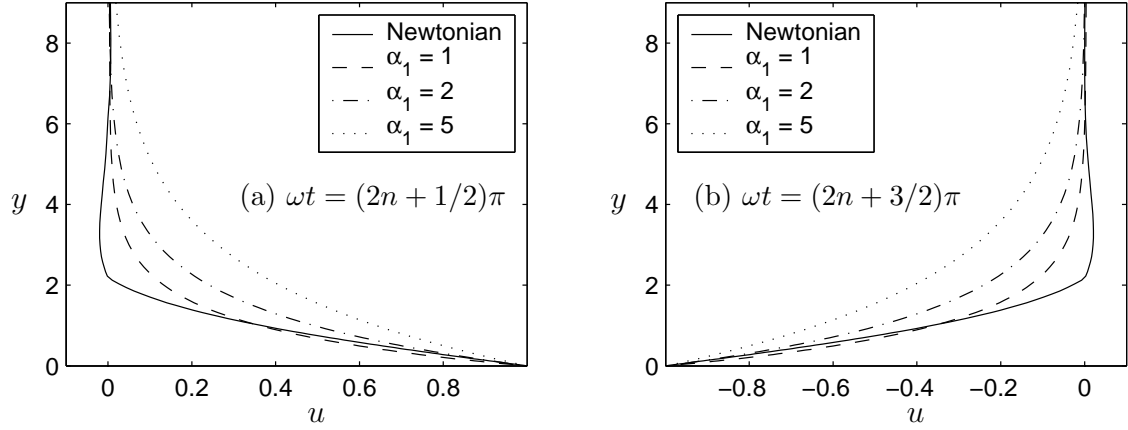


Figure 3: Profiles of the flow velocity $u(y, t)$ at two different time slices $\omega t = (2n + 1/2)\pi$ (left panel) and $\omega t = (2n + 3/2)\pi$ (right panel) for the Newtonian fluid (solid lines) and the fourth-grade non-Newtonian fluid with various values of the second-order material parameter, $\alpha_1 = 1, 2, 5$, while the other high-order material parameters are fixed, $\beta = \beta_1 = \gamma = \gamma_1 = 1$. Here n is chosen to be sufficiently large to assure that the periodic flow has been reached. The other parameters are chosen as $B = 0$, $v_0 = 0$ and $\omega = 1$.

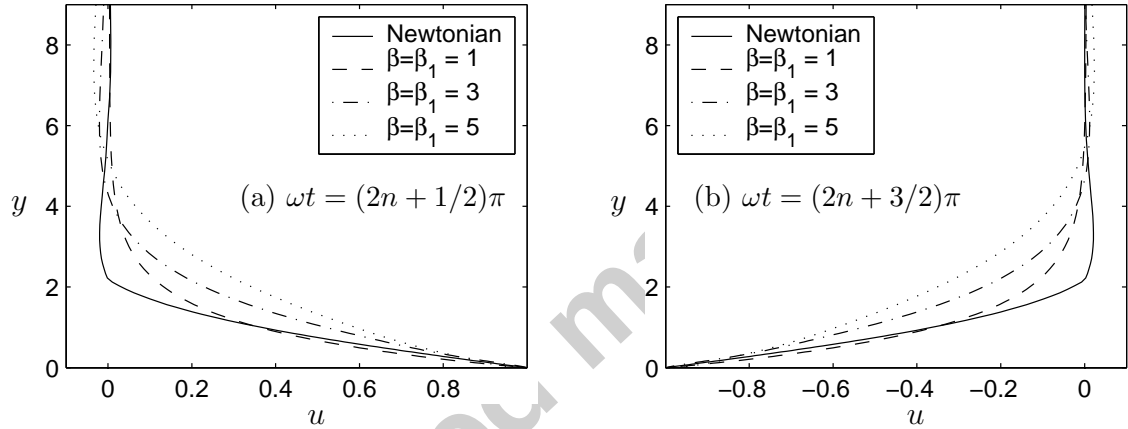


Figure 4: Profiles of the flow velocity $u(y, t)$ at two different time slices $\omega t = (2n + 1/2)\pi$ (left panel) and $\omega t = (2n + 3/2)\pi$ (right panel) for the Newtonian fluid (solid lines) and the fourth-grade non-Newtonian fluid with various values of the third-order material parameters, $\beta = \beta_1 = 1, 3, 5$, while the other high-order material parameters are fixed, $\alpha_1 = \gamma = \gamma_1 = 1$. Here n is chosen to be sufficiently large to assure that the periodic flow has been reached. The other parameters are chosen as $B = 0$, $v_0 = 0$ and $\omega = 1$.

velocity.

To our surprise, an applied magnetic field can put forward the oscillation phase in the domain away from the plate. This can be extracted from the time series of velocity displayed in Fig. 7 for a fourth-grade fluid with three different values of the magnetic field $B = 0, 1, 2$ at two different distances from the plate $y = 1, 2$, respectively. Even a phase lead before the driving plate movement occurs which increases with the increase of the distance away from the plate (by comparing the above and below panels) and the magnetic field strength B , as it can be easily identified in Fig. 7, in which for

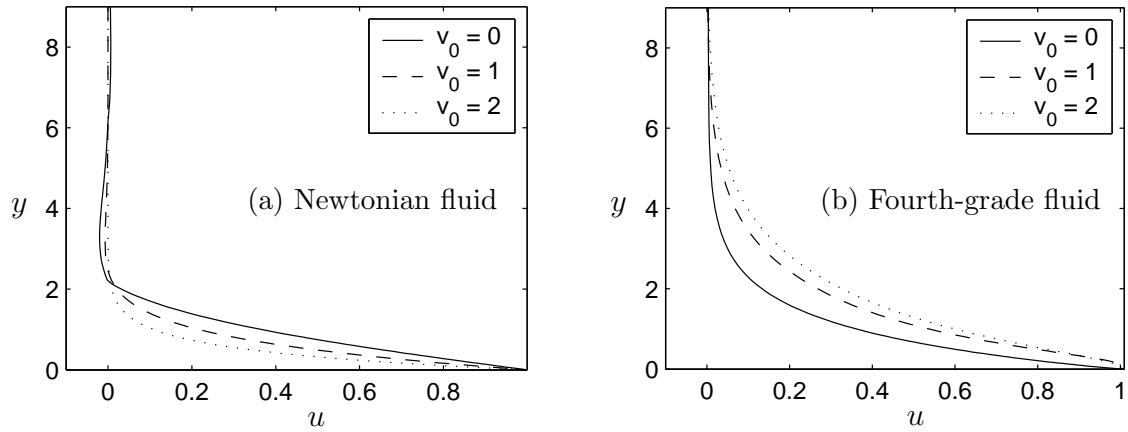


Figure 5: Profiles of the flow velocity $u(y)$ at the time slice $\omega t = (2n + 1/2)\pi$ with a sufficiently large value of n for the Newtonian fluid (left panel) and the fourth-grade fluid $\alpha_1 = \beta = \beta_1 = \gamma = \gamma_1 = 1$ (right panel) with different suction velocities in the absence of the magnetic field $B = 0$. The dimensionless oscillation frequency of the plate is fixed as $\omega = 1$.

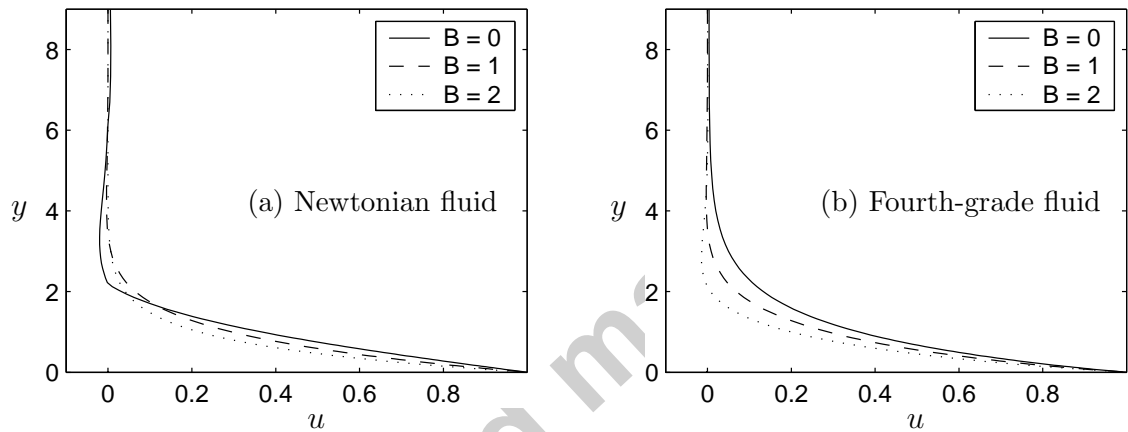


Figure 6: Profiles of the flow velocity $u(y)$ at the time slice $\omega t = (2n + 1/2)\pi$ with a sufficiently large value of n for the Newtonian fluid (left panel) and the fourth-grade fluid $\alpha_1 = \beta = \beta_1 = \gamma = \gamma_1 = 1$ (right panel) with different values of the magnetic field $B = 0, 1, 2$ in the absence of suction/blowing through the plate $v_0 = 0$. The dimensionless oscillation frequency of the plate is fixed as $\omega = 1$.

$B = 0$ (solid lines) the flow is almost in the same phase as the driving plate movement (as shown in Fig. 1). As expected, with the increase of B , the amplitude of the flow decreases because the magnetic force is a resistance to the flow. The influence of B on the velocity time series of a Newtonian fluid has a similar tendency and is not repeated here.

As we have pointed out before, to some extent increasing the high-order material parameters corresponds to the increase of the apparent viscosity of the fourth-grade fluid. This effect can also be seen from the time series of flow velocity at a fixed position $y = 2$ with different values of the second-order material parameter α_1 , displayed in Fig. 8. With the increase of α_1 , the amplitude of the flow velocity at a given distance

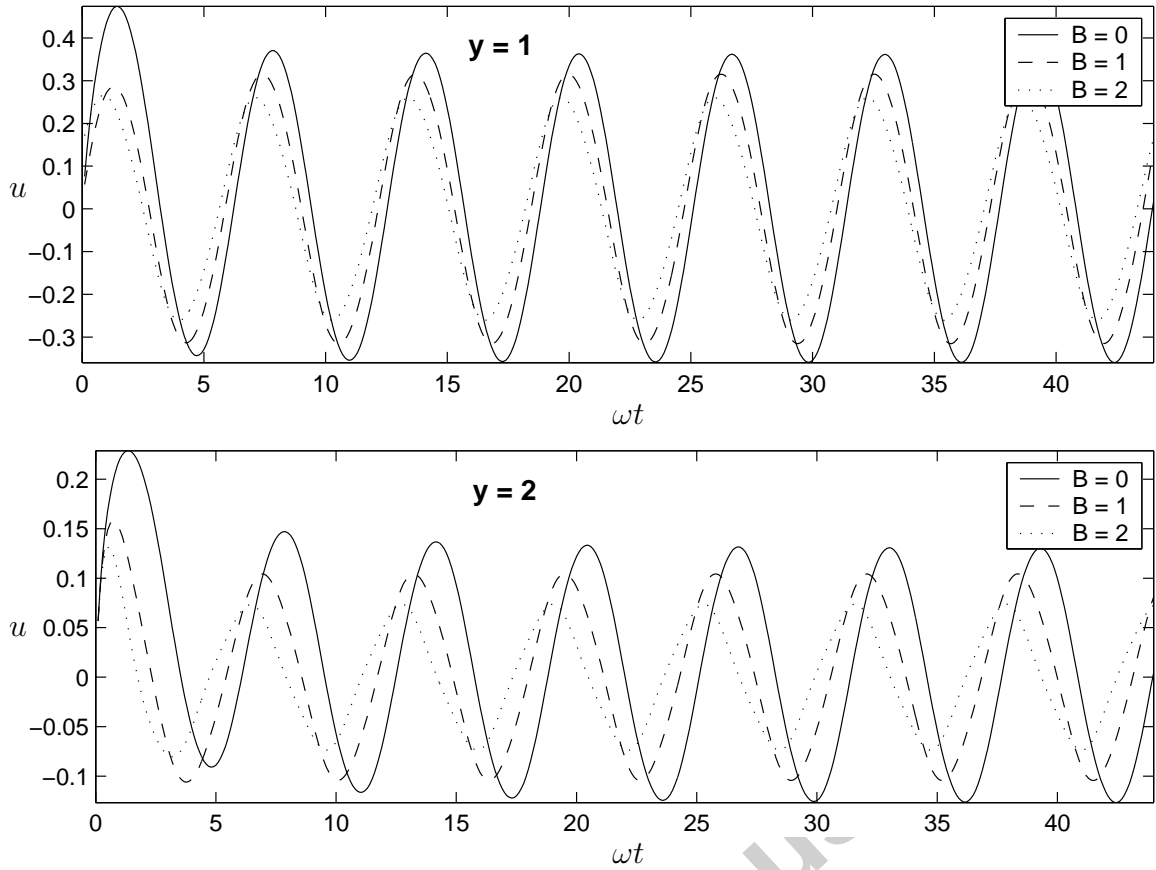


Figure 7: Time series of the flow velocity at two different distances from the plate, $y = 1$ (above panel) and $y = 2$ (below panel), within the first seven periods $\omega t \in [0, 14\pi]$ for a non-Newtonian fluid with the chosen material parameters $\alpha_1 = \beta = \beta_1 = \gamma = \gamma_1 = 1$. For the magnetic field strength, three different values are taken: $B = 0$ (solid lines), $B = 1$ (dashed lines) and $B = 2$ (dotted lines). No suction/blowing past the plate exists $v_0 = 0$. The dimensionless oscillation frequency of the plate is fixed as $\omega = 1$.

from the plate increases, indicating the boundary layer becomes thicker. For cases in which a phase difference between the flow and the driving force occurs, increasing the high-order material parameters will cause the fluid to react to the driving force more rapidly and hence reduce the possible phase difference (lag or lead). This is the case for $B = 2$ displayed in Fig. 8 (below panel), in which the phase lead decreases with the increase of α_1 , whilst for the case of $B = 0$ (the above panel of Fig. 8) the flow velocities with the different values of α_1 are nearly in the same phase with the driving movement, hence such a phase change by varying α_1 is invisible. Numerical results by increasing the other high-order material parameters β , β_1 or γ , γ_1 show similar influences, but are not graphically presented here.

In the numerical results displayed before we took the dimensionless oscillation frequency of the plate as $\omega = 1$. It is fairly interesting to observe the effect of various values of ω on the time series of the velocity and the structure of the boundary layer near the oscillating plate. The corresponding numerical results for three different values

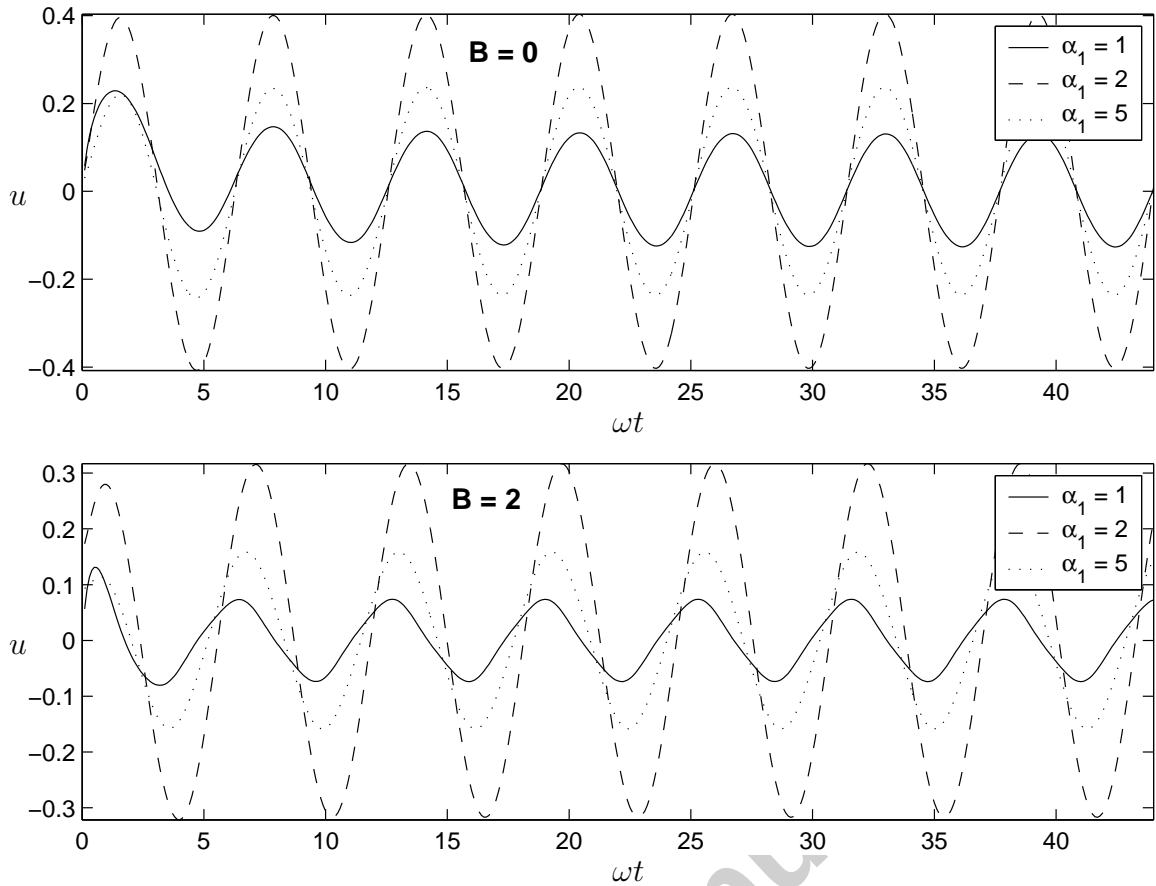


Figure 8: Time series of the flow velocity at a fixed distance from the plate of $y = 2$ within the first seven periods $\omega t \in [0, 14\pi]$ for fourth-grade non-Newtonian fluids with different values of the second-order material parameter α_1 : $\alpha_1 = 1$ (solid line), $\alpha_1 = 2$ (dashed line) and $\alpha_1 = 5$ (dotted line). The values of the other material parameters are fixed: $\beta = \beta_1 = \gamma = \gamma_1 = 1$. The magnetic field strength is chosen as $B = 0$ (above panel) and $B = 2$ (below panel). No suction/blowing past the plate exists: $v_0 = 0$. The dimensionless oscillation frequency of the plate is fixed as $\omega = 1$.

of ω , $\omega = 0.3, 1, 3$, are graphically shown in Figs. 9 and 10, respectively. It is obvious that, for the investigated fourth-order non-Newtonian fluid, the boundary layer near the oscillating plate becomes thicker when the dimensionless oscillation frequency ω deviates from its value of $\omega = 1$, as seen in Fig. 9. The case with $\omega = 1$ corresponds to the thinnest boundary layer. As shown in Fig. 1, for the investigated fourth-order fluid in the absence of the suction/blowing through the plate ($v_0 = 0$) and the magnetic field ($B = 0$), the flow for $\omega = 1$ in the whole flow domain oscillates approximately in phase with the driving plate movement. It is also the case shown in Fig. 10 with $\omega = 1$ (dashed line). For $\omega < 1$ (solid line) a phase lag after the driving plate movement exists, whilst for $\omega > 1$ even a phase lead occurs.

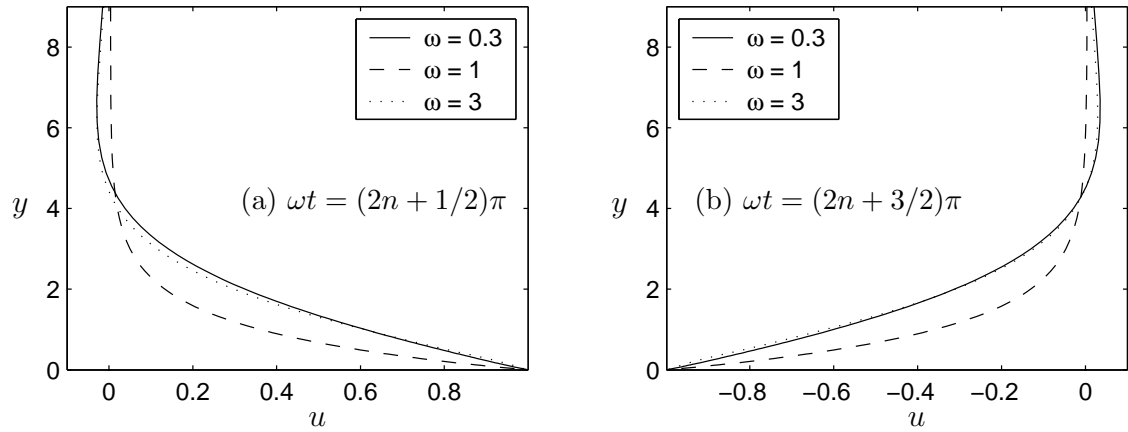


Figure 9: Profiles of the flow velocity $u(y, t)$ at two different time slices $\omega t = (2n + 1/2)\pi$ (left panel) and $\omega t = (2n + 3/2)\pi$ (right panel) for a fourth-grade non-Newtonian fluid with the chosen material parameters $\alpha_1 = \beta = \beta_1 = \gamma = \gamma_1 = 1$. Here n is chosen to be sufficiently large to assure that the periodic flow has been reached. Three different values of the dimensionless frequency ω are considered: $\omega = 0.3, 1, 3$. The other parameters are chosen as $B = 0, v_0 = 0$.

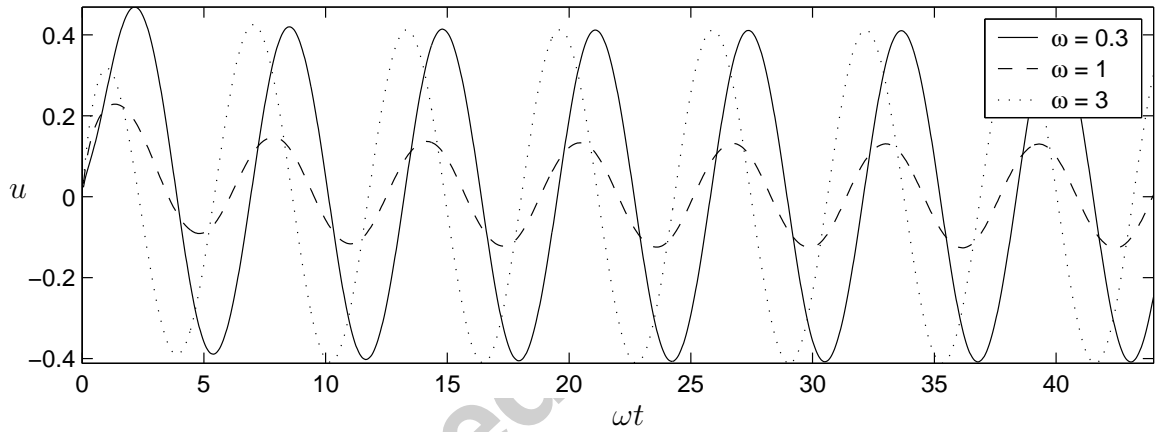


Figure 10: Time series of the flow velocity at a fixed distance from the plate of $y = 2$ within the first seven periods $\omega t \in [0, 14\pi]$ for a fourth-order non-Newtonian fluid with the chosen material parameters $\alpha_1 = \beta = \beta_1 = \gamma = \gamma_1 = 1$. Three different values of the dimensionless frequency ω are taken: $\omega = 0.3, 1, 3$. There exists neither suction/blowing past the plate ($v_0 = 0$) nor external magnetic field ($B = 0$).

5 Final Remarks

The time-dependent flow field of a magnetohydrodynamic (MHD) fluid of grade four is investigated. The velocity field is governed by a non-linear higher-order, sixth-order in space and third-order in time, partial differential equation. The governing equation is sufficiently general to incorporate the effects of an applied magnetic field and allows the study of blowing/suction at the boundary. Numerical results for the unsteady MHD flow caused by a periodic motion of the infinite two-dimensional plate are presented,

for which the surrounding fluid occupies a semi-infinite space. This offers difficulties due to the unbounded domain and the lack of sufficient physical boundary conditions, even in the case of the second- or third-grade fluids, more boundary conditions are necessary in addition to the usual ones for a Newtonian fluid. In the unbounded domain the additional boundary conditions are augmented by enforcing additional asymptotic structure at infinity, although these are relatively weak and physically plausible, see [15]. In order to circumvent the difficulty with the infinite flow domain, a coordinate transformation is employed, which causes some complicated derivations. Furthermore, to match the unsymmetrical boundary conditions, non-central difference schemes for the high-order spatial derivatives are constructed and used.

The purpose of our analysis is to investigate flows of a fourth-grade fluid with a view towards understanding its response characteristics. The flow fields of the fourth-order non-Newtonian fluid are compared with those of a linear Newtonian fluid. Numerical results show that phase differences in flow fields may appear, which may be a phase lag or lead, depending on the chosen parameters. Increasing the strength of the applied magnetic field decreases the boundary-layer thickness, that is valid for both the Newtonian fluid and the fourth-order non-Newtonian fluid, while the effect of alteration in suction velocity through the porous plate shows obvious differences between the Newtonian and fourth-grade non-Newtonian fluids. In general, the fourth-order non-Newtonian fluid exhibits a thicker boundary layer than the Newtonian fluid, and increasing the high-order material parameters of the non-Newtonian fluid causes further thickening of the boundary layer.

It should be pointed out that the quantitative behaviour of high-order fluids is strongly dependent on the choice of the material parameters. At the present time there appears to be no experimental data determining these parameters, particularly for these material parameters in a theory of fourth-order fluids. In this paper, only the simplest prototype flow problem, containing the ingredients essential to understanding the phenomena, is presented. It is only a step towards understanding the behaviour of fourth-order fluids. A good deal of refinement and extension is required, especially the determination of physically reasonable high-order material parameters, before more quantitative answers can be expected.

References

- [1] F. T. Akyildiz: A note on the flow of a non-Newtonian fluid film, *Int. J. Non-Linear Mech.* **33** (1998) 1061–1067
- [2] G. S. Beavers and D. D. Joseph: The rotating rod viscometer, *J. Fluid Mech.* **69** (1975) 475–511.
- [3] A. M. Benharbit and A. M. Siddiqui: Certain solutions of the planar motion of a second grade fluid for steady and unsteady cases, *Acta Mech.* **94** (1992) 85–96.
- [4] C. Bruce, Ph.D. dissertation, Department of Chemical Engineering, Stanford University, CA. (1969).

- [5] J. E. Dunn and K. R. Rajagopal: Fluids of differential type: critical review and thermodynamic analysis, *Int. J. Engng. Sci.* **33** (1995) 689–729.
- [6] M. E. Erdogan: Plane surface suddenly set in motion in a non-Newtonian fluid, *Acta Mech.* **108** (1995) 179–187.
- [7] G. Gupta and M. Massoudi: Flow of a generalized second grade fluid between heated plates, *Acta Mech.* **99** (1993) 21–33.
- [8] T. Hayat, S. Nadeem, S. Asghar and A. M. Siddiqui: Fluctuating flow of a third grade fluid on a porous plate in a rotating medium, *Int. J. Nonlinear Mech.* **36** (2001) 901–916.
- [9] T. Hayat, Y. Wang, A. M. Siddiqui, K. Hutter and S. Asghar: Peristaltic transport of a third-order fluid in a circular cylindrical tube. *Math. Models Methods Appl. Sci.* **12** (2002) 1691–1706.
- [10] T. Hayat, Y. Wang and K. Hutter: Flow of fourth-order fluid. *Math. Models and Methods in Appl. Sci.* **12** (2002) 797–811.
- [11] D. D. Joseph, G. S. Beavers and R. L. Fosdick: The free surface on a liquid between cylinders rotating at different speeds, *Arch. Rat. Mech. Anal.* **49** (1973) 321–401.
- [12] P. N. Kaloni and A. M. Siddiqui: A note on the flow of a viscoelastic fluid between eccentric disks, *J. Non-Newtonian Fluid Mech.* **26** (1987) 125–133.
- [13] J. B. McLeod and K. R. Rajagopal: On the uniqueness of flow of the Navier-Stokes fluid due to a stretching boundary, *Arch. Rat. Mech. Anal.* **98** (1987) 385–394.
- [14] K. R. Rajagopal: On the creeping flow of second order fluid, *J. Non-Newtonian Fluid Mech.* **48** (1984) 239–246.
- [15] K. R. Rajagopal and A. S. Gupta: An exact solution for the flow of a non-Newtonian fluid past an infinite porous plate, *Meccanica* **19** (1984) 158–160.
- [16] C. Truesdell and W. Noll: *The Non-Linear Field Theories of Mechanics*, 2nd edition (Springer, 1992).
- [17] Y. Wang and T. Hayat: Hydromagnetic rotating flow of a fourth-order fluid past a porous plate. *Math. Meth. Appl. Sci.* **27** (2004) 477–496.
- [18] Y. Wang, T. Hayat and K. Hutter: On nonlinear magnetohydrodynamic problems of an Oldroyd 6-constant fluid. *Int. J. Non-Linear Mech.* **40** (2005) 49–58.